Interannual Variability of the Winter North Atlantic Storm Track in CMIP5 Models

Minghao Yang[1], Ruiting Zuo[1], Liqiong Wang[1, 2], Xiong Chen[1], Yanke Tan[3], and Xin Li[1]
[1]*College of Meteorology and Oceanography*, *National University of Defense Technology*, *Nanjing*, *China*
[2]*Nanjing Star-jelly Environmental Consultants Co. Ltd.*, *Nanjing*, *China*
[3]*Institute of Atmospheric Sciences*, *Fudan University*, *Shanghai*, *China*

Abstract

Based on 55-yr output data from the historical runs of twelve Coupled Model Intercomparison Project (CMIP) phase 5 (CMIP5) models and a NCEP (National Centers for Environmental Prediction) reanalysis, we evaluate the capability of those models to simulate the interannual variability of the winter North Atlantic storm track (WNAST). It is found that the multi-model ensemble (MME) is better than any single models in reflecting the spatial distribution of WNAST interannual variability and has the smallest root mean square error (RMSE). The strengths of the interannual variations in half of the models are universally weaker than in the NCEP reanalysis. In addition, the simulated interannual variability vary largely among these models in (55°N−65°N, 35°W−0°). MPI-ESM-LR, FGOALS-s2 and MRI-CGCM3 have relatively better abilities than other models to reflect the interannual variability of WNAST strength, longitude and latitude indices respectively. However, the interannual variability of WNAST longitude and latitude indices (strength index) are (is) overestimated (underestimated) in MME.

(**Citation**: Yang, M., R. Zuo, L. Wang, X. Chen, Y. Tan, and X. Li, 2018: Interannual variability of the winter North Atlantic storm track in CMIP5 models. *SOLA*, **14**, 74−78, doi:10.2151/sola.2018-013.)

1. Introduction

At the end of the 1970s, Blackmon (1976) and Blackmon et al. (1977) found that the synoptic scale (2.5-6 d) transient eddy activity at middle latitudes in the Northern Hemisphere shows two activity centers over the North Pacific and the North Atlantic, respectively, which have been defined as the North Pacific storm tracks (NPST) and the North Atlantic storm tracks (NAST) (Chang et al. 2002). Because the storm tracks can bring about poleward transports of heat, momentum and water vapor, they can greatly influence the maintenance of large scale atmospheric circulation, weather and climate change. On the other hand, the abnormal activities of storm tracks are accompanied by abnormal variations in planetary-scale airflow (Cai and Mak 1990; Branstator 1995), which leads to low frequency variations at mid-latitudes (Luo et al. 2011). Therefore, systematic changes in the intensities and locations of the storm tracks will lead to significant changes in extratropical weather and climate. Here, we focus on the NAST, which could affect not only the United States and Europe, but also, to a certain extent, the Siberian high and East Asia cold surges (Zeng et al. 2015; Zhou et al. 2015).

With the rapid development of climate system models, using them to study and predict the impacts of storm tracks on climate anomalies has become an important approach (Yin 2005; Ulbrich et al. 2008). However, many uncertainties remain in the models, and the differences among the models are large. Therefore, evaluating the simulation capability of a model to simulate storm tracks and analyzing the simulation deviation are of great scientific significance for improving the model itself and for studying and predicting storm tracks. The outputs from the latest climate system models for Coupled Model Intercomparison Project (CMIP) phase 5 (CMIP5) have been extensively investigated. Compared with CMIP3 models, CMIP5 models have higher resolutions, more sophisticated physical processes and better representations of the earth system (Chang et al. 2012; Gong et al. 2014). In terms of using the CMIP models to study storm tracks, Ulbrich et al. (2008) investigated the winter storm track activity over the Northern Hemisphere and its changes in a greenhouse gas scenario based on 13 CMIP3 models. Zappa et al. (2013) evaluated the abilities of 22 CMIP5 models to simulate NAST in winter and summer, which was also compared with CMIP3 models, and found that systematic biases affected the simulated WNAST in these CMIP5 models. Ciasto et al. (2016) used 3 CMIP5 models to research the sensitivity of the NAST to future changes in local and global sea surface temperature.

It can be seen that previous studies placed more emphasis on the scenario projection of storm tracks but hardly involved the interannual variability of the storm tracks, which is closely associated with the variation of jet stream and the transports of heat, momentum and water vapor (Chang 2005). Therefore, we have used 12 CMIP5 models to undertake a more comprehensive study of the interannual variability of the WNAST, which could make efforts using CMIP5 models to study storm tracks more complete and provide a reference for comparisons between the models and further improvements to them. The layout of this paper is as follows. Section 2 describes the data and the analysis methods. Section 3 presents the results. Conclusions are provided in Section 4.

2. Data and methods

Brief information about the 12 CMIP5 models used in this article is provided in Table 1. Considering the outputs data resolutions vary between the models, we first interpolated all the data into a 2.5° × 2.5° grid to facilitate comparison between the models and the NCEP reanalysis. The Lanzcos bandpass filter was used to isolate synoptic scale (2.5−6-day) disturbances from the daily data. Subsequently, the variance of the 500 hPa filtered geopotential height field for the period 1950−2005 was used to represent the storm track. In this study, the winter refers to the time period of December to February.

The method proposed by Li et al. (2011) to define storm track indices, which can represent the WNAST dynamically and quantitatively, was used in this article. Specifically, we set a threshold that is the median of the WNAST strengths of all the grids within a domain (30°N−70°N, 110°W−0°). By doing so, the number of grids was the same for all the samples, and WNAST was well represented by the selected grids. The mean of the values greater than that threshold in all the grids is defined as the strength index of WNAST; conveniently, the average longitude/latitude is defined as the longitude/latitude index. Strength, longitude and latitude indices are expressed as:

$$strength\ index = \frac{1}{N}\sum_{1}^{N} Str, \tag{1}$$

Corresponding author: Ruiting Zuo, National University of Defense Technology, College of Meteorology and Oceanography, No.60, Shuanglong Rd., Jiangning District, Nanjing, China. E-mail: zuoruiting_dw@126.com.

Table 1. List of 12 selected Coupled Model Intercomparison Project (CMIP) phase 5 (CMIP5) climate models.

Model Name	Modeling Group	Atmospheric Resolution (longitude × latitude)
ACCESS1-3 (Australian Community Climate and Earth-System Simulator, version 1−3)	CSIRO and BoM, Australia	192 × 145
CanESM2 (Second Generation Canadian Earth System Model)	CCCma, Canada	128 × 64
CMCC-CM (Centro Euro-Mediterraneo per I Cambiamenti Climatici Climate Model)	CMCC, Italy	480 × 240
CNRM-CM5 (Centre National de Recherches Météorologiques Coupled Global Climate Model, version 5)	Centre National de RecherchesMétéorologiques and Centre Europeen de Recherche et Formation Avancees en Calcul Scientifique, France	256 × 128
FGOALS-g2 (Flexible Global Ocean-Atmosphere-Land System Model (FGOALS) gridpoint, version 2)	LASG, IAP, Chinese Academy of Sciences, China	128 × 64
FGOALS-s2 (FGOALS, second spectral version)	LASG, IAP, Chinese Academy of Sciences, China	128 × 108
GFDL-CM3 (Geophysical Fluid Dynamics Laboratory Climate Model, version 3)	GFDL, NOAA, United States	144 × 90
IPSL-CM5B-LR (L'Institut Pierre-Simon Laplace Coupled Model, version 5B, coupled with NEMO, low resolution)	IPSL, France	96 × 96
MIROC5 (Model for Interdisciplinary Research on Climate, version 5)	Atmosphere and Ocean Research Institute (University of Tokyo), National Institute for Environmental Studies, and Japan Agency for Marine-Earth Science and Technology, Japan	256 × 128
MPI-ESM-LR (Max Planck Institute Earth System Model, low resolution)	MPI for Meteorology, Germany	192 × 96
MRI-CGCM3 (Meteorological Research Institute Coupled Atmosphere–Ocean General Circulation Model, version 3)	Meteorological Research Institute, Japan	320 × 160
NorESM1-M (Norwegian Earth System Model, version 1 (intermediate resolution))	Norwegian Climate Centre, Norway	144 × 96

$$longitude\ index = \frac{1}{N}\sum_{1}^{N} Lon, \text{ and} \tag{2}$$

$$latitude\ index = \frac{1}{N}\sum_{1}^{N} Lat, \tag{3}$$

N is the number of grid points on which the strengths exceed the median of WNAST strength of all the grids within a domain. *Str*, *Lon* and *Lat* then are the strength, longitude and latitude of the WNAST at that grid point, respectively. A positive difference with NCEP in latitude (longitude) index means a northward (eastward) shift of the storm track in CMIP5.

3. Results

3.1 Interannual variability

In this section, the interannual standard deviation of WNAST strength is used as a metric to evaluate the models' abilities to simulate the interannual variations of the WNAST. Figure 1 shows the interannual standard deviations and the climatology of WNAST strength based on the NCEP reanalysis and the MME and their differences. The interannual variation of the WNAST in the NCEP reanalysis shows spatial structure of the double center (Fig. 1a). The two centers are located in (52.5°N, 45°W) and (65°N, 30°W), and the center strengths both exceed 900 gpm^2. However, there is only one center in the MME (Fig. 1b), located in (50°N, 55°W), and the center strength is weaker than that in the NCEP reanalysis. In addition, the interannual variation in the MME is universally underestimated, and the absolute value of the deviation center exceeds 150 gpm^2. As for the climatology of WNAST, the center spatial structure in the MME (Fig. 1c) is nearly consistent with the NCEP reanalysis (Fig. 1d) and the spatial correlation coefficient between the climatology in the NCEP reanalysis and that in the MME is 0.98. However, the climatology in the MME, similar to the simulated interannual variations, is also universally underestimated.

Although the MME can basically capture the features of the WNAST interannual variations, the simulated results vary by model. Figure 2 shows the interannual standard deviations of the WNAST amplitude (shading) and the differences with the NCEP reanalysis (contours) in the 12 CMIP5 models. As seen from Fig. 2, there are significant differences in the interannual variations of WNAST amplitude in the models. Five models (CMCC-CM, FGOALS-g2, IPSL-CM5B-LR, MIROC5 and MRI-CGCM3) successfully simulate the double center structure. Almost all the models have greater or smaller simulation deviations for the position of the south-western center, but the simulation result in IPSL-CM5B-LR is similar to the NCEP reanalysis. In addition, 5 models (IPSL-CM5B-LR, FGOALS-g2, ACCESS1-3, MIROC5 and CMCC-CM) can reproduce the location of the north-east center, and CMCC-CM could well simulate the center strength.

To clearly delineate the performance of each model in simulating the WNAST, Taylor diagrams (Fig. 3) (Taylor 2001) are plotted to concisely display the relative information from the multiple models. As seen from Fig. 3, the spatial correlation coefficients of FGOALS-g2, ACCESS1-3 and IPSL-CM5B-LR with the NCEP reanalysis are all 0.94, which shows a relatively better ability than other models for simulating the spatial distribution of interannual variations of WNAST amplitude, whereas the spatial correlation coefficients in the other five models (CanESM2, MPI-ESM-LR, CMCC-CM, MRI-CGCM3 and CNRM-CM5) are less than 0.9. It is worth noting that the spatial correlation coefficient between the MME and NCEP reanalysis is 0.96, and the root mean square error

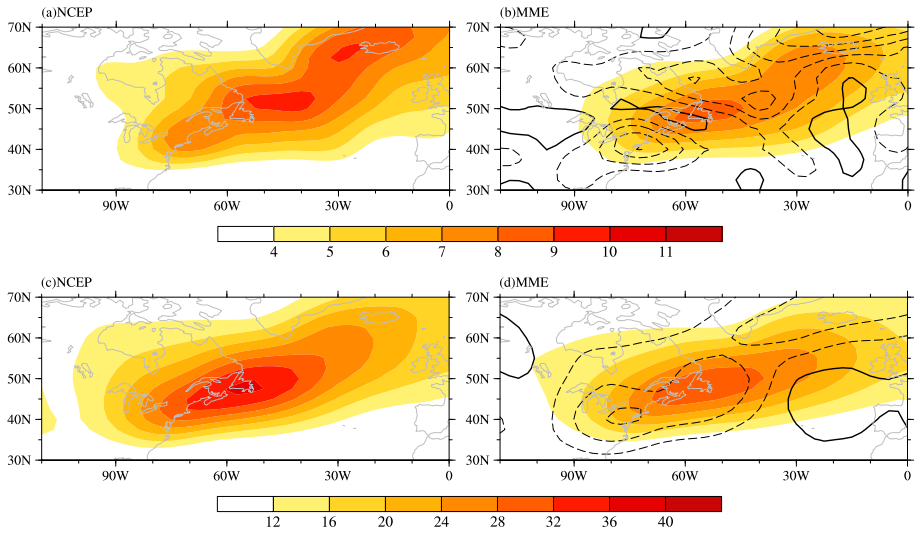

Fig. 1. Interannual standard deviations of the WNAST amplitudes (shading) derived from (a) the NCEP reanalysis and (b) the multi-model ensemble (MME), and climatology (shading) derived from (c) NCEP reanalysis and (d) MME, and the difference between MME and NCEP reanalysis (contour in (b) and (d), with an interval of 0.5 and 2 respectively, black bold line represents the contour with the zero value) (units: 100 gpm^2).

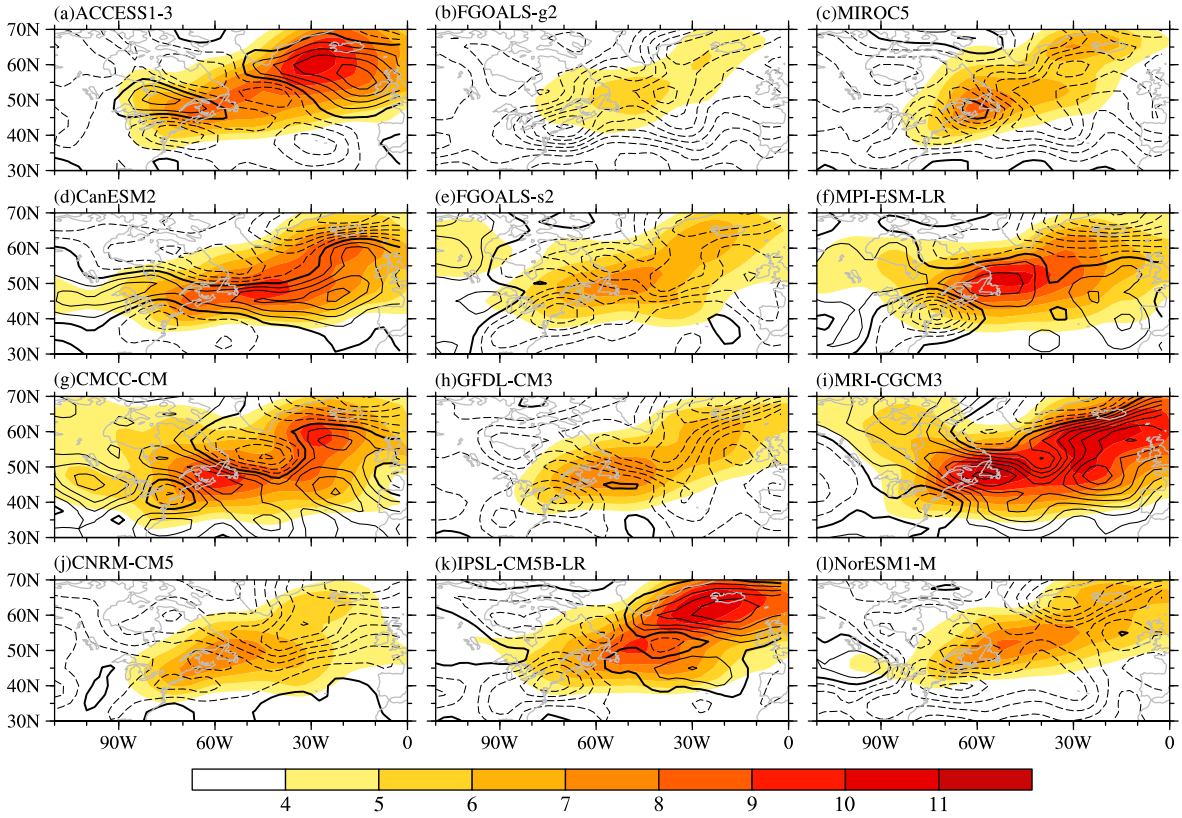

Fig. 2. Interannual standard deviations of the WNAST amplitudes (shading) in individual CMIP5 models and its difference from the NCEP reanalysis (contours with intervals of 0.5; the bold black line represents the zero-value contour) (units: 100 gpm^2).

(RMSE) is smaller than that in a single model, indicating that the MME has a better ability to simulate the spatial distribution of interannual variations of WNAST amplitude, but the simulated standard deviation of interannual variation of WNAST amplitude in the MME is smaller than that in the NCEP reanalysis.

It is found that the strengths of the interannual variation of WNAST amplitude in half of the models (FGOALS-g2, FGOALS-s2, MIROC5, GFDL-CM3, CNRM-CM5 and NorESM1-M) are universally weaker than that in the NCEP reanalysis. The strength of the north-east center is overestimated in three of the models (ACCESS1-3, MRI-CGCM3 and IPSL-CM5B-LR), especially that in MRI-CGCM3. With the exception of CanESM2, CMCC-CM and IPSL-CM5B-LR, the south-west center strengths in which are close to that in the NCEP reanalysis, the simulation results in the majority of models are underestimated, and only those in MPI-ESM-LR and MRI-CGCM3 are better. As seen from Fig. 3, the RMSEs in FGOALS-g2, CanESM2, MRI-CGCM3 and CNRM-CM5 are relatively large, especially that in MRI-CGCM3,

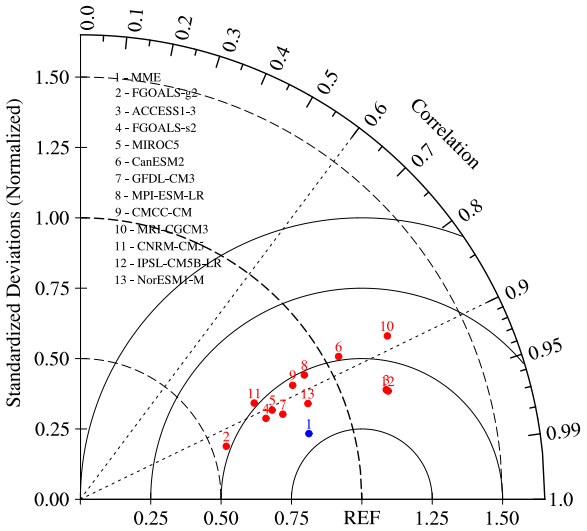

Fig. 3. Taylor diagram of WNAST interannual variations.

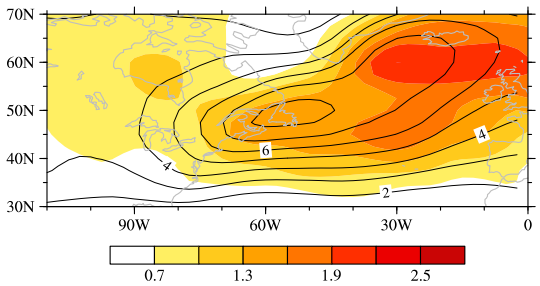

Fig. 4. Standard deviations (spread) of the CMIP5 models (shading), and the contour is the MME of the simulated WNAST amplitudes of interannual variability.

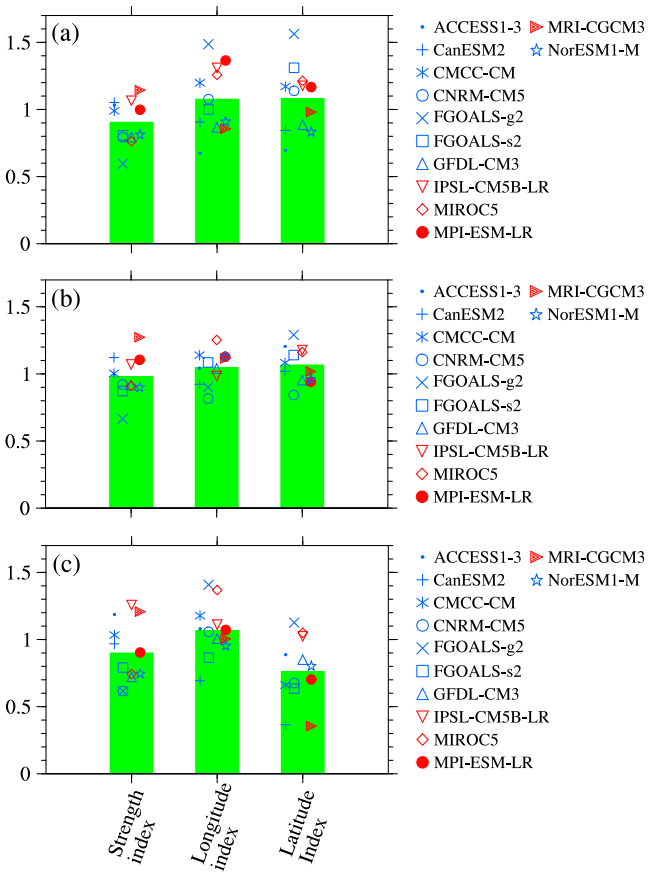

Fig. 5. Ratios of the interannual standard deviations of the indices in each model over whole domain (a), south-western peak region (45°N−55°N, 70°W−30°W) (b) and north-eastern peak region (55°N−70°N, 40°W−10°W) (c) to those in the NCEP reanalysis. The green bars represent the MME of the corresponding indices.

but those in ACCESS1-3 and IPSL-CM5B-LR were smaller than in other models, indicating, to a certain extent, a better ability to simulate the intensity of the interannual variations of WNAST. The standard deviations of the interannual variations of WNAST amplitude are well reproduced in CanESM2 but overestimated in four of the models (ACCESS1-3, CanESM2, MRI-CGCM3 and IPSL-CM5B-LR) and underestimated in the remaining models. In addition, the simulated standard deviations of the interannual variations in FGOALS-g2 have the greatest differences with those in the NCEP reanalysis.

To assess the differences in WNAST interannual variations in these models, Fig. 4 shows the intermodel spreads estimated with the standard deviations among the 12 CMIP5 models, which clearly reflects the regional differences among the models. The differences between the models are primarily concentrated in (55°N−65°N, 35°W−0°) where the simulation results of the WNAST climatology vary largely among the models.

3.2 Characteristic indices related to the WNAST

To further evaluate the ability of these CMIP5 models to simulate the interannual variation of the WNAST, Fig. 5 shows the ratios of the interannual standard deviations of the three characteristic indices related to the WNAST in the CMIP5 models to those in NCEP reanalysis. The closer the ratio is to 1, the better the ability to simulate interannual variation. As seen from Fig. 5a, the interannual variation of winter strength index in most of the models, especially FGOALS-g2, is smaller than that in the NCEP reanalysis. MME also underestimate the interannual variation of winter strength index, whereas a quarter of the models (CanESM2, IPSL-CM5B and MRI-CGCM3) overestimate that. The interannual variations in winter strength index in ACCESS1-3, CMCC-CM and especially MPI-ESM-LR are basically in accordance with the NCEP reanalysis, indicating a relatively better simulation ability. The interannual variation of winter longitude index in FGOALS-s2 is nearly the same as the NCEP reanalysis, which means that this model could be used as an indicator to reflect the interannual variation of winter longitude index. In addition, among these 12 CMIP5 models, MRI-CGCM3 can well simulate the interannual variation in winter latitude index. Although the simulation result for the interannual variation in winter strength index in ACCESS1-3 is satisfactory, that model was nearly unable to reproduce the interannual variation in winter longitude/ latitude index due to the huge difference between the NCEP reanalysis. The interannual variations in the three characteristic indices related to the WNAST in FGOALS-g2 have the maximum simulation deviations, showing that it can hardly be used to measure the interannual variation of the WNAST.

To evaluate adequately the double peak structure (Fig. 1a), the two peak regions, the south-western side (45°N−55°N, 70°W−30°W) and north-eastern side (55°N−70°N, 40°W−10°W), are evaluated separately (Figs. 5b and 5c). It can be seen that the capability to simulate the interannual variation of characteristic indices over two peak regions differs obviously among these CMIP5 models. In general, the ratios in the south-western side of WNAST are closer to 1 than that in the north-eastern side. In addition, the MME in the south-western side is almost consistent with the NCEP reanalysis, which indicate that CMIP5 models have a better capability to simulate the interannual variation of the south-western side WNAST.

4. Conclusion and discussion

Based on 55-yr output data from historical runs of 12 CMIP5 models and NCEP reanalysis, this study presents a relatively comprehensive evaluation of the interannual variability of the WNAST in these the CMIP5 models. The main conclusions are as follows.

In terms of interannual variability, there are two centers in the NCEP reanalysis, but there is only one center in MME and in more than half of the models. MME not only has a better ability to simulate the spatial distribution of interannual variation than any single model but also the smallest RMSE. The simulation results in ACCESS1-3 and IPSL-CM5B-LR are also satisfactory. The strengths in the interannual variations in half of the models and MME are universally underestimated. The spatial standard deviation of interannual variation is well reproduced in CanESM2, whereas FGOALS-g2 has the largest simulation deviation. The simulations results of interannual variation vary largely among these models in (55°N−65°N, 35°W−0°).

The interannual variation of WNAST strength index is underestimated in majority of the models. MPI-ESM-LR, FGOALS-s2 and MRI-CGCM3 have relatively better abilities than other models to reflect the interannual variability of WNAST strength, longitude and latitude indices respectively, while FGOALS-g2 can hardly be used as an indicator to reflect the interannual variation of the WNAST. The MME overestimate the interannual variation of WNAST longitude and latitude indices but underestimate that of strength index.

Although these selected CMIP5 models can well simulate the basic characteristics of the interannual variation the WNAST, some deficiencies remain. For example, the interannual variability of the WNAST in approximately half of the models are overall weaker than that in the NCEP reanalysis. Recently, Shaw et al. (2016) reviewed the research work on storm tracks and emphasized that under the background of global warming and due to a series of thermodynamic changes caused by the increase in carbon dioxide concentration, the intensities and locations of storm tracks have changed. The climate change caused by the increase in carbon dioxide concentration may have influence on the interannual variability of WNAST, and this is what we are planning to explore. In addition, it is noted that in the first part of the NCEP reanalysis (before 1979) there were few satellite data included. This may have had an impact on the comparing among these CMIP5 models.

Acknowledgements

We thank Fujun Qi for valuable discussions and encouragement. We thank the World Climate Research Programme for providing the CMIP5 data, which could be found at https://esgf-node.llnl.gov/search/cmip5/. The NCEP Reanalysis were obtained from NOAA and are available at http://www.esrl.noaa.gov/psd/data/gridded/. This research was supported by National Natural Science Foundation of China (41490642, 41605051, 41475070).

Edited by: M. Sugi

Reference

Blackmon, M. L., 1976: A climatological spectral study of the 500 mb geopotential height of the Northern Hemisphere. *J. Atmos. Sci.*, **33**, 1607−1623.

Blackmon, M. L., and co-authors, 1977: An observational study of the Northern Hemisphere wintertime circulation. *J. Atmos. Sci.*, **34**, 1040−1053.

Branstator, G., 1995: Organization of storm track anomalies by recurring low-frequency circulation anomalies. *J. Atmos. Sci.*, **52**, 207−226.

Cai, M., and M. Mak, 1990: Symbiotic relation between planetary and synoptic scale waves. *J. Atmos. Sci.*, **47**, 2953−2968.

Chang, E. K. M., and Y. Fu, 2002: Interdecadal variations in Northern Hemisphere winter storm track intensity. *J. Climate*, **15**, 642−658.

Chang, E. K. M., 2005: An idealized nonlinear model of the Northern Hemisphere winter storm tracks. *J. Atmos. Sci.*, **63**, 1818−1839.

Chang, E. K. M., Y. Guo, and X. Xia, 2012: CMIP5 multi-model ensemble projection of storm track change under global warming. *J. Geophys. Res.*, **117**, D23118.

Ciasto, L. M., and co-authors, 2016: North Atlantic storm-track sensitivity to projected sea surface temperature: Local versus remote influences. *J. Climate*, **29**, 6973−6991.

Gong, H., and co-authors, 2014: The climatology and interannual variability of the East Asian winter monsoon in CMIP5 models. *J. Climate*, **27**, 1659−1678.

Li, Y., W. Zhu, and J. Wei, 2010: Reappraisal and improvement of winter storm track indices in the North Pacific. *Chin. J. Atmos. Sci.*, **34**, 1001−1010 (in Chinese).

Luo, D., Y. Diao, and S. B. Feldstein, 2011: The variability of the Atlantic storm track and the North Atlantic Oscillation: A link between intraseasonal and interannual variability. *J. Atmos. Sci.*, **68**, 577−601.

Shaw, T. A., and co-authors, 2016: Storm track processes andthe opposing influences of climate change. *Nature Geosci.*, **9**, 656−664.

Taylor, K. E., 2001: Summarizing multiple aspects of model performance in a single diagram. *J. Geophys. Res. Atmos.*, **106**, 7183−7192.

Yin, J. H., 2005: A consistent poleward shift of the storm tracks in simulations of 21st century climate. *Geophys. Res. Lett.*, **32**, L18701.

Ulbrich, U., and co-authors, 2008: Changing Northern Hemisphere storm tracks in an ensemble of IPCC climate change simulations. *J. Climate*, **21**, 1669−1679.

Zappa, G., L. C. Shaffrey, and K. I. Hodges, 2013: The ability of CMIP5 models to simulate North Atlantic extratropical cyclones. *J. Climate*, **26**, 5379−5396.

Zeng, D., and co-authors, 2015: North Atlantic storm track and its influence on Siberian High in winter. *Trans. Atmos. Sci.*, **38**, 232−240 (in Chinese).

Zhou, X., W. Zhu, and C. Gu, 2015: Possible influence of the variation of the northern Atlantic storm track on the activity of cold waves in China during winter. *Chin. J. Atmos. Sci.*, **39**, 978−990 (in Chinese).

Manuscript received 25 March 2018, accepted 5 June 2018
SOLA: https://www.jstage.jst.go.jp/browse/sola/